Role of the primary motor cortex in L-DOPA-induced dyskinesia and its modulation by 5-HT1A receptor stimulation

Corinne Y Ostock[a], **Kristin B Dupre**[a], **Karen L Eskow Jaunarajs**[a], **Hannah Walters**[a], **Jessica George**[a], **David Krolewski**[b], **Paul D Walker**[b], and **Christopher Bishop**[a,*]

Corinne Y Ostock: costock1@binghamton.edu; Kristin B Dupre: kdupre1@binghamton.edu; Karen L Eskow Jaunarajs: keskow1@binghamton.edu; Hannah Walters: hwalter1@binghamton.edu; Jessica George: JGeorge7@binghamton.edu; David Krolewski: dkrolews@umich.edu; Paul D Walker: pdwalker@med.wayne.edu; Christopher Bishop: cbishop@binghamton.edu

[a] Behavioral Neuroscience Program, Department of Psychology, Binghamton University, Binghamton, NY 13902-6000, USA

[b] Department of Anatomy and Cell Biology, Wayne State University School of Medicine, Detroit, MI 48201, USA

Abstract

While serotonin 5-HT1A receptor (5-HT1AR) agonists reduce L-DOPA-induced dyskinesias (LID) by normalizing activity in the basal ganglia neurocircuitry, recent evidence suggests putative 5-HT1AR within the primary motor cortex (M1) may also contribute. To better characterize this possible mechanism, c-fos immunohistochemistry was first used to determine the effects of systemic administration of the full 5-HT1AR agonist ±8-OH-DPAT on L-DOPA-induced immediate early gene expression within M1 and the prefrontal cortex (PFC) of rats with unilateral medial forebrain bundle (MFB) dopamine (DA) lesions. Next, in order to determine if direct stimulation of 5-HT1AR within M1 attenuates the onset of LID, rats with MFB lesions were tested for L-DOPA-induced abnormal involuntary movements (AIMs) and rotations following M1 microinfusions of ±8-OH-DPAT with or without co-administration of the 5-HT1AR antagonist WAY100635. Finally, ±8-OH-DPAT was infused into M1 at peak dyskinesia to determine if 5-HT1AR stimulation attenuates established L-DOPA-induced AIMs and rotations. While no treatment effects were seen within the PFC, systemic ±8-OH-DPAT suppressed L-DOPA-induced c-fos within M1. Intra-M1 5-HT1AR stimulation diminished the onset of AIMs and this effect was reversed by WAY100635 indicating receptor specific effects. Finally, continuous infusion of ±8-OH-DPAT into M1 at peak dyskinesia alleviated L-DOPA-induced AIMs. Collectively, these findings support an integral role for M1 in LID and its modulation by local 5-HT1AR.

Keywords

primary motor cortex; Parkinson's disease; L-DOPA-induced dyskinesia; serotonin; c-fos

*Corresponding Author: Christopher Bishop, Ph.D., Department of Psychology, Binghamton University, 4400 Vestal Parkway East, Binghamton, NY 13902, Phone: (607) 777-3410, Fax: (607) 777-4890, cbishop@binghamton.edu.

Introduction

Chronic dopamine (DA) replacement therapy with L-DOPA for the treatment of Parkinson's disease (PD) often leads to the development of L-DOPA-induced dyskinesias (LID) which are characterized by abnormal involuntary movements (AIMs; Jankovic, 2005). One possible mechanism underlying the development of LID involves the dysregulation of DA release from serotonin (5-HT) neurons (Carta et al., 2007). Indeed, following DA depletion, 5-HT neurons from the raphe nucleus convert exogenous L-DOPA to DA and release it into the striatum (Arai et al., 1994; Navailles et al., 2010). In line with these findings, serotonin 1A receptor (5-HT1AR) agonists likely reduce LID in both experimental and clinical populations by tempering supraphysiological striatal DA levels through stimulation of inhibitory somatodendritic 5-HT1A autoreceptors (Bara-Jimenez et al., 2005; Bibbiani et al., 2001; Carta et al., 2007; Eskow et al., 2009; Lindgren et al., 2010).

While evidence has implicated the dorsal raphe nucleus (Carta et al., 2007; Eskow et al., 2009) as a target for 5-HT1AR agonists, additional research suggests that extra-raphe 5-HT1AR within the basal ganglia circuitry may also modulate the expression of LID (Dupre et al., 2007; Iravani et al., 2006). For example, direct stimulation of 5-HT1AR within the subthalamic nucleus (STN; Marin et al., 2009) and the striatum has been shown to decrease L-DOPA (Bishop et al., 2009) and DA agonist (Dupre et al., 2008) induced dyskinesias without adversely affecting anti-parkinsonian efficacy. Interestingly, a population of post-synaptic cortical 5-HT1AR known to influence corticostriatal signaling is upregulated following MPTP lesions in macaques and persists throughout L-DOPA treatment (Huot et al., 2010). Furthermore, functional imaging studies have revealed overactivity in the primary motor cortex (M1) in humans during the expression of LID (Rasol et al., 1998). Therefore, it is possible that stimulation of 5-HT1AR within M1 may diminish the onset and expression of LID.

In order to characterize the cellular, functional, and anatomical specificity of 5-HT1AR effects in the cortex, we investigated the effects of systemic ±8-OH-DPAT following L-DOPA administration on c-fos expression within M1 and the prefrontal cortex (PFC) of unilateral 6-OHDA lesioned rats. Next, the effects of intracortical 5-HT1AR stimulation in M1 on both the onset and peak expression of LID were examined using microinfusion and microdialysis techniques, respectively. The present results suggest the importance of M1 in LID and implicate its modulation through 5-HT1AR stimulation as a therapeutic target for the attenuation of LID.

2. Material and methods

2.1 Animals

Adult male Sprague-Dawley rats were used (N = 44; 225–250 g upon arrival; Taconic Farms, Hudson, NY, USA). Animals were housed in plastic cages (22 cm high, 45 cm deep, and 23 cm wide) and had free access to water and standard lab chow (Rodent Diet 5001; Lab Diet, Brentwood, MO, USA). The colony room was maintained on a 12/12 h light/dark cycle (lights on at 0700 hs) at a temperature of 22–23°C. Animals were treated in accordance with the guidelines of the Institutional Animal Care and Use Committee of Binghamton University and the "Guide for the Care and Use of Laboratory Animals" (Institute of Laboratory Animal Resources, National Academic Press 1996; NIH publication number 85-23, revised 1996).

2.2 Experiment 1: Effect of systemic ±8-OH-DPAT and L-DOPA on cortical c-fos and ALO AIMs expression

2.2.1 Medial forebrain 6-hydroxydopamine lesion surgery—The first study investigated the effect of systemic ±8-OH-DPAT on L-DOPA-induced cortical c-fos expression in L-DOPA-primed rats (n = 11, 3–4 rats/group). One week after arrival, rats received unilateral 6-hydroxydopamine (6-OHDA; 3 μg/μl; Sigma) lesions of the left medial forebrain bundle (MFB). Desipramine HCl (25 mg/kg, ip) was administered 20 min prior to surgery in order to protect noradrenergic neurons. Rats were anesthetized with inhalant isoflurane (2–3%) in oxygen (2.5 L/min) and placed in a stereotaxic apparatus. The following coordinates relative to bregma were used for the 6-OHDA injection site: AP, −1.8 mm; ML, +2.0 mm; DV, −8.6 mm with the incisor bar positioned at 5.0 mm below interaural line (Paxinos & Watson, 1998). After drilling a small hole in the skull above the coordinates, a 26 gauge needle attached to a 10 μl Hamilton syringe containing 6-OHDA dissolved in 0.9% NaCl + 0.1% ascorbic acid was lowered into the MFB. A total of 4 μl was injected at a rate of 2 μl/min and the needle was withdrawn 5 min later. Stainless steel wound clips were used to close the surgical site and animals were placed in clean cages (2 per cage). Five min pre-surgery and 1 h and 1 day post-surgery, rats received an injection of buprenorphine HCL (0.03 mg/kg ip; Rechitt Benckiser Pharmaceuticals Inc., Richmond, VA). Wound clips were removed 1 week post-surgery. Animals were handled twice per week for 3 weeks to ensure full recovery and acclimation to experimental procedures.

2.2.2 Pharmacological treatments—Three weeks following surgery, rats were primed with L-DOPA methyl ester (12 mg/kg, ip) + DL-serine 2-(2,3,4-trihydroxybenzyl) hydrazide hydrochloride (Benserazide, 15 mg/kg, ip; Sigma) for 7 consecutive days to induce stable LID (Bishop et al., 2009; Dupre et al., 2011; Eskow et al., 2007). Rats were split into equally dyskinetic groups based on axial, limb, and orolingual (ALO) AIMs ratings (see description below) on the fifth day of L-DOPA priming, and were subsequently randomly assigned to receive 1 of 3 treatment combinations on day 8: Vehicle (0.9% NaCl, ip) followed 5 min later by Vehicle (0.9% NaCl containing 0.1% ascorbic acid, ip), Vehicle followed 5 min later by L-DOPA (12 mg/kg, ip) or the full 5-HT1AR agonist ±8-OH-DPAT (1.0 mg/kg, ip) 5 min prior to L-DOPA (12 mg/kg, ip). Rats were observed for ALO AIMs 20, 40, and 60 min following injections after which they were immediately anesthetized and perfused for immunohistochemical analysis of M1 and PFC c-fos expression (see description below).

2.3 Experiment 2: Effect of Intra-M1 ±8-OH-DPAT on the onset of ALO AIMs

2.3.1. MFB 6-hydroxydopamine lesion and cannulae implantation surgeries—
In order to characterize the effects of direct 5-HT1AR stimulation within M1 on the onset of dyskinesia, Experiment 2 investigated the effects of intra-M1 infusions of ±8-OH-DPAT on AIMs and rotations in hemiparkinsonian rats. Rats (n = 23) received unilateral MFB 6-OHDA lesions using the same procedure described in Experiment 1. During the same surgery, rats were also implanted with 22 gauge guide cannulae (C313G/SPC; Plastics One Inc., Roanoke, VA) into M1 ipsilateral to the DA lesion. With the incisor bar located 5.0 mm below the interaural line, 14 mm cannulae were positioned within M1 using the following coordinates: AP, +2.2 mm; ML, +2.5 mm; DV, −1.5 mm relative to bregma (Paxinos & Watson, 1998). Cannulae were fixed in place using dental acrylic (Lang Dental, Wheeling, IL) and 4 screws. Dummy cannulae (Plastics One) cut 1 mm shorter than the guide cannulae were inserted in the guide cannulae to preserve patency. Animals were then single housed in clean cages with access to water and standard lab chow. Rats were handled and habituated to the microinjection procedure once per week for 3 weeks following surgery.

2.3.2. Pharmacological treatments—Three weeks after surgery, rats were primed for 7 consecutive days with L-DOPA (12 mg/kg, + Benserazide 15 mg/kg, sc). On days 1, 4, and 7 of priming, ALO AIMs and contralateral rotations were observed immediately after injections every 10 min for 2 h. Rats displaying an ALO AIMs score of ≥ 30 by the 7th day of priming, which corresponds with at least 95% striatal DA depletion upon reverse-phase high performance liquid chromatography coupled to electrochemical detection (HPLC-ED) analysis (Eskow et al., 2007), were retained for further analysis (n=19). Intracortical microinfusions began 2 days after the last day of L-DOPA priming, and test days occurred every 2–3 days. The first group of rats (n = 12) received 1 of 3 intracortical pretreatments per test day in a within-subjects counterbalanced order: Vehicle (0.9% NaCl) or 2 different doses of ±8-OH-DPAT (1 or 10 μg; Sigma). In the second group, also using the same within-subjects counterbalanced design, rats (n = 7) received 1 of 4 intracortical pretreatments: Vehicle (0.9% NaCl), ±8-OH-DPAT (10 μg), the 5-HT1AR antagonist N-[2-[4-(2-Methoxyphenyl)-1-piperazinyl]ethyl]-N-2-pyridinylcyclohexanecarboxamide maleate salt (WAY100635; 5 μg; Sigma), or combined ±8-OH-DPAT (10 μg) + WAY100635 (5 μg). Preliminary test infusions with cresyl violet dye in a separate set of rats confirmed that the placement and volume of infusion were appropriately located within M1. During infusions, rats were restrained with a towel and a 15 mm injector (Plastics One) was lowered to 1 mm past the end of the guide cannula. Drugs were infused at a rate of 0.5 μl/min for a total of 1.0 μl using a microinfusion pump (Harvard Apparatus, Boston, MA) that held one 10 μl Hamilton syringe attached to plastic tubing (PE20 Tygon tubing; Plastics One) and the injector. Following infusions, the injector was left in place for an additional 2 min. Five min following intra-M1 injections, rats received systemic injections of L-DOPA (12 mg/kg + Benserazide, 15 mg/kg, sc) and were then monitored for ALO AIMs and rotations every 10 min for 2 h. A post-test with L-DOPA alone was performed at the end of the study and ensured stable AIMs throughout testing (mean sum ALO AIMs: Day 7 of priming = 60 ±1.6, post-test = 59 ±1.5; p > 0.05).

2.4 Experiment 3: Effect of Intra-M1 ±8-OH-DPAT on peak ALO AIMs expression

2.4.1. MFB 6-hydroxydopamine lesion and cannulae implantation surgeries—
In order to determine if intra-M1 5-HT1AR stimulation attenuates established LID, the third experiment investigated the effects of intra-cortical ±8-OH-DPAT infusions during peak LID on ALO AIMs and rotations. Rats (n = 10) received unilateral MFB 6-OHDA lesions using the same procedure described in Experiment 1. During the same surgery, rats were fitted unilaterally with plastic microdialysis guide cannulae (CMA 12 Elite; Stockholm, Sweden) targeting M1 ipsilateral to the DA lesion (AP, +2.2 mm; ML, +2.5 mm; DV, −1.5 mm relative to bregma; Paxinos & Watson, 1998). Cannulae were fixed in place using dental acrylic (Lang Dental, Wheeling, IL) and 4 screws. Animals were then single housed in clean cages with access to water and standard lab chow. Rats were handled and habituated to the microdialysis procedure once per week for 3 weeks following surgery.

2.3.2. Pharmacological treatments—Three weeks after surgery, rats were primed for 7 consecutive days with L-DOPA (12 mg/kg, + Benserazide 15 mg/kg, sc). On the final day of priming, ALO AIMs and contralateral rotations were observed every 10 min for 3 h and rats displaying an ALO AIMs score of ≥ 30 by the 7th day of priming were retained for further analysis (n=9). Reverse phase microdialysis testing began 2 days after the last day of L-DOPA priming. On test days, unilateral microdialysis probes (CMA 12 Elite; 1mm membrane length; 20 000 Dalton; Stockholm, Sweden) were introduced so that the dialysis membrane extended −1.5 to −2.5 ventral to bregma within M1 ipsilateral to the lesion. The probes were perfused with artificial cerebral spinal fluid (aCSF; in mM: 128 NaCl, 2.5 KCl, 1.3 $CaCl_2$, 2.1 $MgCl_2$, 0.9 NaH_2PO_4, and 1.0 glucose, brought to a pH of 7.4) at a constant flow rate of 2 μl/min for 120 min. Following this, rats received systemic injections of L-

DOPA (12 mg/kg + Benserazide, 15 mg/kg, sc). Sixty min post L-DOPA administration, corresponding with peak dyskinesia (Lundblad et al., 2002; Dupre et al., 2007), Vehicle (aCSF) or ±8-OH-DPAT (5 or 20 mM) was perfused into M1 for 60 min. ALO AIMs and rotations were monitored every 10 min for 3 h immediately following L-DOPA treatment.

2.5. Behavioral Analyses

2.5.1. Abnormal Involuntary Movements (AIMs)—Rats were monitored for AIMs using a procedure described by Bishop et al. (2006). On test days (0900 – 1400 h), rats were individually placed in plastic cylinders 5 min prior to pretreatments. Following L-DOPA injection, trained observers blind to treatment condition assessed each rat for exhibition of axial, limb, and orolingual (ALO) AIMs. In addition, contralateral rotations, defined as complete 360° turns away from the lesioned side of the brain, were tallied. Ipsilateral rotations were not observed. 'Axial' AIMs were characterized by dystonic posturing of the neck and torso, involving positioning of the neck and torso in a twisted manner directed toward the side of the body contralateral to the lesion. 'Limb' AIMs were defined as rapid, purposeless movements of the forelimb located on the side of the body contralateral to the lesion. 'Orolingual' AIMs were composed of repetitive openings and closings of the jaw and tongue protrusions. The movements were considered abnormal as they occurred at times when the rats were not chewing or gnawing on food or other objects. Every 10th or 20th min for up to 180 min, rats were observed for 2 consecutive min. Rats were rated for AIMs during the 1st min and rotational behavior in the 2nd min. During the AIMs observation period, a severity score of 0–4 was assigned for each AIMs category: 0, not present; 1, present for <50% of the observation period (i.e. 1–29 s); 2, present for >50% of the observation period (i.e. 30–59 s); 3, present for the entire observation period (i.e. 60 s) and interrupted by a loud stimulus (a tap on the wire cage lid), or 4, present for the entire observation period but not interrupted by a loud stimulus.

2.6. Histology and Neurochemical Analyses

2.6.1. C-fos immunohistochemistry—Using a similar procedure as Bishop et al. (2009), 1 h after treatment, rats in Experiment 1 were deeply anesthetized with ketamine (90 mg/kg, ip) + xylaxine (50 mg/kg, ip) (Lloyd Laboratories, Shenendoah, IA) and transcardially perfused with 0.1 M phosphate-buffered saline (PBS) at pH 7.4 after fixation with 4% paraformaldehyde in 0.1 M PBS, pH 7.4. Brains were removed and stored in perfusion buffer at 4°C for at least 2 days before cutting 50-μm-thick sections on a vibratome 100 μm apart. Once cut, free-floating immunohistochemistry using standard avidin-biotin-peroxidase complex (ABC) detection methods was performed. Sections were incubated in 0.3% H_2O_2 in 0.1 M PBS (30 min) to block endogenous peroxidases and subsequently exposed to blocking buffer containing 0.3% Triton X-100, 1% normal goat serum, 1% bovine serum albumin, and 0.05% sodium azide in 0.01 M PBS, pH 7.4 (60 min) to reduce nonspecific antibody binding. Sections were then incubated in blocking buffer containing polyclonal rabbit anti-c-fos primary antibody (sc-52; Santa Cruz, CA) at 1–5000 overnight at 4°C. The sections were then successively treated with blocking buffer containing rat preabsorbed biotinylated goat anti-rabbit (Chemicon International, CA) at 1–500 (2 h) and then ABC (Elite Vectastain Kit; Vector Laboratories, CA) diluted 1–500 in 0.01 M PBS containing 0.02% Triton X-100 (60 min). Chromagen was visualized with 0.005% 3,3diaminobenzidine (Sigma), 0.6% nickel ammonium sulfate, and 0.005% H_2O_2 in 0.05 M Tris-HCl, pH 7.6. Light microscopic analysis was performed under bright-field optics with a Zeiss Axioscope microscope (Zeiss, Oberkochen, Germany) fitted with a Spot RT camera (Diagnostic Instruments, Inc., Sterling Heights, MI). Digitized images for analyses were obtained from serial sections taken from M1 (at approximately +2.2 AP to bregma) and PFC (at approximately +2.7 AP to bregma; Paxinos & Watson, 1998). As described in Bishop et al. (2009) cortical images representing 1 mm^2 area were processed as

8-bit grayscale TIFF files by ImageJ software (NIH) by first sharpening to enhance nuclear detail and then adjusting the threshold to separate positive stained nuclei from background where necessary. For all cortical regions, threshold objects were automatically counted on both sides (lesioned and intact) and expressed as the number of c-fos positive cells ± SEM. Manual count comparisons with several images were used to verify accuracy of these methods. All images were precoded and analyzed without knowledge of specific pharmacological treatment.

2.6.2. Tissue dissection and cryostat sectioning—Three days after experiments were completed, rats in Experiments 2 and 3 were sacrificed by decapitation and brains were immediately removed. To determine the level of DA depletion, posterior striata from rats in Experiment 3 were freshly dissected, frozen at −80°C and subjected to monoamine analysis using high-performance liquid chromatography (HPLC-ED, see description below). The primary motor cortices from rats in Experiments 2 and 3 were also examined for verification of intracortical cannulation placements. To accomplish this, whole brains from Experiment 2 and anterior portions of the brain from Experiment 3 were removed and rapidly frozen in methylbutane (−30°C) and stored at −20°C. Cresyl violet (FD Neurotechnologies, Baltimore, MD) staining was used to determine injection sites in cryostat-generated 20 mm coronal sections containing injection sites that were post-fixed with 4% paraformaldehyde (Fisher Scientific, Hanover Park, IL). All animals had cannulae placements within M1 (see Fig. 2A, B for representative placements).

2.6.3 High-performance liquid chromatography—HPLC-ED was conducted on striatal tissue, obtained from rats in Experiment 3, according to the protocol of Eskow et al. (2007). Samples were homogenized in ice-cold perchloric acid (0.1 M) with 1% ethanol and 0.02% EDTA. The homogenates were spun for 30 min at 14,000 g with the temperature maintained at 4°C. Aliquots of supernatant were then analyzed for abundance of DA and 3,4-dihydroxyphenylacetic acid (DOPAC), 5-HT, and 5-hydroxyindole-3-acetic acid (5-HIAA) via HPLC-ED. The final oxidation current values were compared to known standards $10^{-6} - 10^{-9}$, adjusted to striatal tissue weights, and expressed as percent intact ±S.E.M.

2.7. Data Analyses

In Experiment 1, immunohistochemistry was analyzed using a one-way ANOVA. Planned comparison post hoc tests were used for analysis of c-fos main effects. Treatment effects (expressed as means ± S.E.M.) for ALO AIMs were analyzed by using non-parametric Kruskal Wallis tests in Experiments 1 and 3. Significant differences between treatments were examined using Mann Whitney U post hoc comparisons for ALO AIMs. In Experiment 2, treatment effects for ALO AIMs and rotations were analyzed using non-parametric Friedman ANOVAs and two-way repeated-measures ANOVAs with both time and treatment as within-subject factors, respectively. Significant differences between treatments were examined using a selected number of Wilcoxon post hoc comparisons for ALO AIMs and planned comparisons for rotations when appropriate. Rotations in the third experiment were analyzed using two way mixed design ANOVAs with time as a within-subjects factor and treatment as a between-subjects factor. Monoamine and metabolite levels in the striatum from Experiment 3 were analyzed using paired t-tests (comparing intact vs. lesioned striata). Analyses were performed with the use of Statistica software '98 (Statsoft Inc., Tulsa, OK, USA) and alpha was set at $p < 0.05$.

3. Results

3.1. Experiment 1: Systemic ±8-OH-DPAT reduces L-DOPA-induced ALO AIMs and M1 c-fos expression

5-HT1AR agonist treatment has previously been shown to reduce LID (Bishop et al., 2009; Eskow et al., 2007; Lindgren et al., 2010). In the current study, behavioral analyses of LID also revealed a main effect of treatment for ALO AIMs ($H_2 = 8.2663$, $p < 0.05$; Fig. 1B). L-DOPA treatment increased ALO AIMs compared to vehicle treatment while systemic adjunct treatment with the 5-HT1AR agonist, ±8-OH-DPAT attenuated ALO AIMs in L-DOPA-treated, DA-depleted rats (all $p < 0.05$). However, it is unknown how 5-HT1AR agonists affect cellular markers of neuronal activity in M1, the primary excitatory input to the striatum. Therefore, immunohistochemistry for the immediate early gene, c-fos was used to determine the effects of both L-DOPA treatment and coincident stimulation of 5-HT1AR on cortical neuronal activity. Analysis of c-fos expression on the non-depleted contralateral side did not yield significant effects of treatment in either M1 or PFC (data not shown, $p > 0.05$). On the lesioned ipsilateral side, L-DOPA treatment significantly increased M1 c-fos expression but no changes were observed within the PFC ($F_{2,8} = 30.9184$, $p < 0.01$; Fig. 1A, C, D). Within M1, pretreatment with ±8-OH-DPAT significantly attenuated the L-DOPA-induced increase in c-fos expression ($p < 0.05$). These results indicate a site-specific activation of M1 neurons following L-DOPA treatment in DA-depleted rats that is attenuated by systemic 5-HT1AR stimulation.

3.2. Experiment 2: Intra-M1 ±8-OH-DPAT dose and receptor dependently reduces the onset of ALO AIMs

M1 is a major contributor of excitatory innervation to the striatum (Antonelli et al., 2005). However, the precise role of M1 5-HT1AR in the anti-dyskinetic effects of 5-HT1AR agonists has yet to be determined. To clarify this, ±8-OH-DPAT was directly infused into M1 of hemiparkinsonian, L-DOPA-primed rats through chronically implanted cannulae followed by a systemic injection of L-DOPA. Immediately following L-DOPA injection, contralateral rotations and ALO AIMs were monitored every 10 min for 2 h. While there was no effect of treatment on rotations, a significant interaction between treatment and time was found ($F_{22,242} = 1.881$, $p < 0.05$; Fig. 3D) and indicated a differential effect of the high dose of ±8-OH-DPAT on rotational activity. For example, the high dose of ±8-OH-DPAT decreased rotations at the 20th min compared to all treatments and increased rotations at the 40th min compared to Vehicle, while increasing rotations at the 110th min compared to the low dose of ±8-OH-DPAT (all $p < 0.05$).

Direct infusions of ±8-OH-DPAT into M1 reduced the onset of dyskinesia in the first hour for axial (min 20, 30, & 40: $\chi^2 = 18.05$, 11.45, and 9.80 respectively, all $p < 0.05$; Fig. 3A) forelimb (min 20, 30, 40: $\chi^2 = 19.95$, 12.00, and 9.33 respectively, all $p < 0.05$; Fig. 3B) and orolingual (min 20, 30: $\chi^2 = 10.89$ and 9.59 respectively, all $p < 0.05$; Fig. 3C) AIMs. The effects of intra-M1 ±8-OH-DPAT were also dose-dependent. The high dose of ±8-OH-DPAT (10 μg) reduced axial, forelimb, and orolingual AIMs at the 20th and 30th min compared to all treatments and axial and forelimb AIMs at the 40th min compared to Vehicle (all $p < 0.05$). The low dose (1 μg) also reduced axial AIMs compared to Vehicle at the 40th min ($p < 0.05$). These results are the first to directly confirm the integral role of M1 in the anti-dyskinetic effects of 5-HT1AR agonists.

In order to determine receptor specificity of ±8-OH-DPAT for the 5-HT1AR, the full 5-HT1AR antagonist WAY100635 (5 μg) was co-infused into M1 along with ±8-OH-DPAT (10 μg) in L-DOPA-treated, DA depleted rats. Again, intra-M1 ±8-OH-DPAT decreased axial (min 30, 40: $\chi^2 = 9.47$ and 11.25, respectively, $p < 0.05$; Fig. 4A), forelimb (min 20,

30, 40: χ^2 = 13.13, 12.06, 10.38 respectively) and orolingual (min 10, 20, 30, 40: χ^2 = 8.23, 10.81, 8.56, and 9.96, p < 0.05; Fig. 4C) AIMs, but not rotations during the first h following L-DOPA treatment (20–40 min; Fig. 4A, B, C). While the 5-HT1AR antagonist, WAY100635 did not affect AIMs, coincident antagonism with WAY100635 reversed the anti-dyskinetic effects of ±8-OH-DPAT microinfusion within M1 (20–40 min; all p > 0.05). These results indicate that ±8-OH-DPAT's effects were specific to the 5-HT1AR.

3.3.1. Experiment 3: Intra-M1 ±8-OH-DPAT reduces peak ALO AIMs—In order to determine whether M1 5-HT1AR stimulation during peak LID attenuates established L-DOPA-induced ALO AIMs and contralateral rotations, Vehicle (aCSF) or ±8-OH-DPAT (5 or 20 mM) was infused into M1 for 60 min starting 1 h after systemic injections of L-DOPA. ALO AIMs and contralateral rotations were monitored every 10 min for 3 h following L-DOPA treatment. Contralateral rotations were modulated by administration of intra-M1 ±8-OH-DPAT at peak dyskinesia. No effect of treatment was found on rotational behavior but there was a significant interaction between treatment and time ($F_{34,238}$ = 1.80, p < .001; Fig. 5B). Continuous stimulation of cortical 5-HT1AR at peak LID attenuated the rotational response of rats during the second h following L-DOPA treatment. Indeed, planned comparisons revealed that the high dose of ±8-OH-DPAT (20 mM) decreased rotations at the 90th – 130th min compared to Vehicle (all p < 0.05) and at the 80th, 100th, and 130th min compared to the low dose of ±8-OH-DPAT (5mM).

Results of a Kruskal-Wallis ANOVA revealed that continuous infusions of ±8-OH-DPAT effectively diminished L-DOPA-induced ALO AIMs expression during the second h (min 80, 90, 110, 120: H_2= 8.70, 7.97, 10.87, and 11.95 respectively; all p < 0.05). As shown in Fig. 5A, the high dose of ±8-OH-DPAT (20 mM) significantly reduced ALO AIMs compared to all treatments at the 90th, 110th, and 120th min (p < 0.05 for all) and to Vehicle at the 50th and 80th min (p < 0.05 for all). These results show that the reduction in ALO AIMs seen following intra-M1 ±8-OH-DPAT administration is not simply due to a shift in the onset of LID.

3.3.2. Monoamine and Metabolite Levels—HPLC-ED analysis demonstrated that unilateral 6-OHDA injections into the MFB significantly reduced striatal DA (t_8 = 8.69, p < 0.001) and DOPAC (t_8 = 9.54, p < 0.001) on the lesioned side by >97% and >98% compared to the intact side, respectively. In this group of rats, 5-HIAA levels were elevated on the lesioned side to 126% (t_8 = −2.82, p < 0.05) but there were no differences between contralateral and ipsilateral striatal 5-HT levels.

4. Discussion

Multiple basal ganglia sites have been associated with the expression and treatment of LID. More recently, evidence has accumulated implicating a more primary role for M1. In the current investigation we provide cellular and functional confirmation of the link between M1 and LID, while further demonstrating that 5-HT1AR agonists convey their anti-dyskinetic efficacy in part via this structure. For the first time we show that L-DOPA-induced ALO AIMs were associated with an increase in c-fos expression in M1 but not the PFC. Furthermore, systemic administration of the selective 5-HT1AR agonist ±8-OH-DPAT reduced L-DOPA-induced AIMs and attenuated c-fos expression within M1. Finally, we show novel evidence that direct stimulation of 5-HT1AR in M1 with ±8-OH-DPAT dose-dependently and receptor-specifically diminished both the onset and peak expression of LID.

C-fos is a biological marker (Herrera & Robertson, 1996; Sheng and Greenberg, 1990) believed to reflect neuronal activation following L-DOPA treatment within the basal

ganglia. Following DA depletion, L-DOPA potently induces expression of this immediate early gene in the striatum (Bishop et al., 2009; Lopez et al., 2001) and STN (Soghomonian, 2006). In the current study we extend previous work, reporting increased c-fos induction in M1 following L-DOPA treatment in DA-depleted, dyskinetic rats (Fig. 1). Notably, these effects were not observed in the PFC which has been implicated in the expression of LID by repetitive transcranial magnetic stimulation (rTMS; Rektorova et al., 2008) and PET imaging (Brooks et al., 2000). L-DOPA's differential cortical effects shown here are supported by anatomical studies showing that electrical stimulation of the PFC activates the ventral striatum, while stimulation of M1 strongly activates the dorsolateral striatum (Glynn & Ahmad, 2002), a region highly implicated in the expression of LID (Cenci et al., 1999). Indeed, L-DOPA treatment induces greater c-fos expression within the dorsal striatum compared to the ventral striatum (Bishop et al., 2009; Mura et al., 2002). Thus, together with the aforementioned studies, our L-DOPA-induced M1 c-fos expression supports the possible role of an overactive corticostriatal mechanism in LID proposed by others (Chase & Oh, 2000).

Next, we report for the first time that systemic coadministration of the 5-HT1AR agonist ±8-OH-DPAT reduces the expression of L-DOPA-induced c-fos within M1 (Fig. 1A and C), while concomitantly reducing ALO AIMs expression (Fig. 1B). These findings complement previous work by our lab showing that ±8-OH-DPAT attenuates the expression of L-DOPA-induced striatal c-fos expression, with the most pronounced effects observed in the dorsal striatum (Bishop et al., 2009). In addition to c-fos, other molecular markers such as ΔFosB have been associated with the expression of LID (Andersson et al., 1999; Cao et al., 2010; Westin et al., 2001). Future studies are warranted as alterations of this marker in M1 have not yet been investigated in LID. Taken as a whole, these results support the possibility that 5-HT1AR agonists may diminish LID, in part, by lessening overactivation of the corticostriatal pathway at its origin and termination.

5-HT1AR stimulation in multiple brain regions has been shown to decrease LID; however, the role of intra-M1 5-HT1AR stimulation on LID has not been previously investigated. Here we show that intracerebral ±8-OH-DPAT effectively reduced the onset of AIMs without affecting rotations during the first hour (Fig. 3 & 4), corresponding to the short half-life of ±8-OH-DPAT in the brain (30–45 min; Yu & Lewander, 1997). Importantly, coinfusion of the full 5-HT1AR antagonist WAY100635 completely reversed these effects (Fig. 4A–C), indicating that the anti-dyskinetic actions were specific to M1 5-HT1AR. Though the magnitude of these effects were less pronounced than those observed following direct infusions of ±8-OH-DPAT into the striatum (Bishop et al., 2009) or the longer acting 5-HT1AR agonist sarizotan into the STN (Marin et al., 2009), continuous infusion of ±8-OH-DPAT into M1 at peak dyskinesia attenuated L-DOPA-induced ALO AIMs and rotations (Fig. 5). Of note, M1 microinfusions of the higher dose of ±8-OH-DPAT (10 μg) briefly produced 5-HT syndrome in some animals, characterized by flat body posture and lower lip retraction. However, this effect wore off prior to the onset of AIMs ratings and is likely not responsible for the reduction seen in ALO AIMs. Furthermore, no animals displayed 5-HT syndrome when ±8-OH-DPAT (5 and 20mM) was continuously infused into M1 during peak L-DOPA-induced AIMs. Finally, while the systemic dose of ±8-OH-DPAT used in the current study produced transient (5–10 min) flat body posture and lower lip retraction, previous work has shown that this dose does not reduce the efficacy of L-DOPA on the forepaw adjusting steps test, a metric of anti-parkinsonian efficacy (Bishop et al., 2009). Collectively, these results suggest that cortical 5-HT1AR stimulation decreases LID but high doses have the potential to causes adverse side effects.

While it has been well established that 5-HT1AR stimulation decreases L-DOPA derived DA release from raphe-striatal neurons (Aria et al., 1994; Carta et al., 2007; Lindgren et al.,

2010), results from the current study suggest an additional post-synaptic mechanism by which 5-HT1AR stimulation decreases LID. Indeed, inhibitory post-synaptic cortical 5-HT1AR located on glutamatergic pyramidal neurons in layer V of the cortex (Pangalos et al., 1992; Pompeiano et al., 1992) project to the striatum (McGeorge & Faull; 1989). 5-HT1AR agonists may convey their anti-LID effect through attenuation of excitatory postsynaptic currents in pyramidal neurons within layer V of the cortex (Aghajanian & Marek, 1997). In line with this, functional imaging studies have revealed overactivity of M1 in humans during the expression of LID (Rascol et al., 1998) and recent evidence suggests that LID is associated with abnormal glutamate signaling in motor areas including M1 and the striatum (Ahmed et al., 2011). Indeed, previous studies have found that following DA denervation, L-DOPA treatment increases both extracellular striatal glutamate levels and dyskinesia (Jonkers, 2002; Robelet et al., 2004; Dupre et al, 2011). While the current study did not directly measure the relationship between M1 5-HT1AR and striatal glutamate in dyskinesia, there is evidence in intact rats that direct stimulation of 5-HT1AR within M1 decreases both cortical and striatal glutamate levels (Antonelli et al., 2005). Moreover, systemic administration of 5-HT1AR agonists has been shown to decrease extracellular striatal glutamate in L-DOPA-treated (Dupre et al., 2011) and L-DOPA-naive (Mignon & Wolf, 2005) hemiparkinsonian rats. Collectively, these findings suggest that the anti-dyskinetic actions of 5-HT1AR may be due in part to modulation of glutamatergic signaling of corticostriatal neurons.

5. Conclusions

The current study provides strong evidence for the role of M1 in LID. Furthermore, we demonstrate that selective stimulation of 5-HT1AR within the motor cortex can attenuate both the onset and expression of peak AIMs. While the anti-dyskinetic effects of cortical 5-HT1AR stimulation likely involves the modulation of the corticostriatal pathway, further studies are necessary in order to elucidate this potential mechanism. In conclusion, the current research highlights a motor cortex-mediated mechanism through which 5-HT1AR agonists work to reduce LID, which may improve the use of these compounds for the treatment of LID.

Acknowledgments

Abbreviations

DA	Dopamine
PD	Parkinson's disease
LID	L-DOPA-induced dyskinesia
5-HT	Serotonin
5-HT1AR	Serotonin 1A receptor
M1	Primary motor cortex
PFC	Prefrontal cortex
AIMS	Abnormal involuntary movements scale
6-OHDA	6-hydroxydopamine
MFB	Medial forebrain bundle

ALO	Axial, Limb, Orolingual
WAY100635	N-[2-[4-(2-Methoxyphenyl)-1-piperazinyl]ethyl]-N-2-pyridinylcyclohexanecarboxamide maleate salt
DPAT	±8-OH-DPAT
Benserazide	DL-serine 2-(2,3,4-trihydroxybenzyl) hydrazide hydrochloride
HPLC-ED	high performance liquid chromatography coupled to electrochemical detection
ABC	avidin-biotin-peroxidase complex
DOPAC	3,4-dihydroxyphenylacetic acid
5-HIAA	5-hydroxyindole-3-acetic acid

References

Aghajanian GK, Marek GJ. Serotonin induces excitatory postsynaptic potentials in apical dendrites of neocortical pyramidal cells. Neuropharmacology. 1997; 36(4/5):589–99. [PubMed: 9225284]

Ahmed I, Bose SK, Pavese N, Ramlackhansingh A, Turkheimer F, Hotton G, Hammers A, Brooks DJ. Glutamate NMDA receptor dysregulation in Parkinson's disease with dyskinesias. Brain. 2011; 134:979–86. [PubMed: 21371994]

Andersson M, Hilbertson A, Cenci MA. Striatal fosB expression is causally linked with l-DOPA-induced abnormal involuntary movements and the associated upregulation of striatal prodynorphin mRNA in a rat model of Parkinson's disease. Neurobiol Dis. 1999; 6:461–474. [PubMed: 10600402]

Antonelli T, Fuxe K, Tomasini MC, Bartoszyk GD, Seyfried CA, Tangenelli S, et al. Effects of Sarizotan on the corticostriatal glutamate pathways. Synapse. 2005; 58:193–199. [PubMed: 16138317]

Arai R, Karasawa N, Geffard M, Nagatsu T, Nagatsu I. Immunohistochemical evidence that central serotonin neurons produce dopamine from exogenous L-DOPA in the rat, with reference to the involvement of aromatic L-amino acid decarboxylase. Brain Res. 1994; 26:295–299. [PubMed: 7697371]

Bara-Jimenez W, Bibbiani F, Morris MJ, Dimitrova T, Sherzai A, Mouradian MM, et al. Effects of serotonin 5-HT1A agonist in advanced Parkinson's disease. Mov Disord. 2005; 20:932–936. [PubMed: 15791634]

Bibbiani F, Oh JD, Chase TN. Serotonin 5-HT1A agonist improves motor complications in rodent and primate parkinsonian models. Neurology. 2001; 57:1829–1834. [PubMed: 11723272]

Bishop C, Taylor JL, Kuhn DM, Eskow KL, Park JL, Walker PD. MDMA and fenfluramine reduce L-DOPA-induced dyskinesia via indirect 5-HT1A receptor stimulation. Eur J Neurosci. 2006; 23:2669–2676. [PubMed: 16817869]

Bishop C, Krolewski DM, Eskow KL, Barnum CJ, Dupre KB, Deak T, et al. Contribution of the striatum to the effects of 5-HT1A receptor stimulation in L-DOPA-treated hemiparkinsonian rats. J Neurosci Res. 2009; 81:1645–1658. [PubMed: 19115412]

Brooks DJ, Piccini P, Turjanski N, Samuel M. Neuroimaging of dyskinesia. Ann Neurol. 2000; 47:S154–158. [PubMed: 10762143]

Calabresi P, Galletti F, Saggese E, Ghiglieri V, Picconi B. Neuronal networks and synaptic plasticity in Parkinson's disease: beyond motor deficits. Parkinsonism Relat Disord. 2007; 13:S259–262. [PubMed: 18267247]

Cao X, Yasuda T, Uthayathas S, Watts RL, Mouradian MM, Mochizuki H, Papa SM. Striatal overexpression of ΔFosB reproduces chronic levodopa-induced involuntary movements. J Neurosci. 2010; 30:7335–7343. [PubMed: 20505100]

Carta M, Carlsson T, Kirik D, Bjorklund A. Dopamine released from 5-HT terminals is the cause of L-DOPA-induced dyskinesia in parkinsonian rats. Brain. 2007; 130:1819–1833. [PubMed: 17452372]

Cenci MA, Lee CS, Björklund A. L-DOPA-induced dyskinesia in the rat is associated with striatal overexpression of prodynorphin- and glutamic acid decarboxylase mRNA. Eur J Neurosci. 1998; 10:2694–2706. [PubMed: 9767399]

Chase TN, Oh JD. Striatal dopamine- and glutamate-mediated dysregulation in experimental parkinsonism. Trends Neurosci. 2000; 23:S86–91. [PubMed: 11052225]

Dupre KB, Eskow KL, Negron G, Bishop C. The differential effects of 5-HT(1A) receptor stimulation on dopamine receptor-mediated abnormal involuntary movements and rotations in the primed hemiparkinsonian rat. Brain Res. 2007; 1158:135–143. [PubMed: 17553470]

Dupre KB, Eskow KL, Barnum CJ, Bishop C. Striatal 5-HT1A receptor stimulation reduces D1 receptor-induced dyskinesia and improves movement in the hemiparkinsonian rat. Neuropharmacology. 2008a:1–8.

Dupre KB, Eskow KL, Steiniger A, Klioueva A, Negron G, Lormand L, et al. Effects of coincident 5-HT1A receptor stimulation and NMDA receptor antagonism on L-DOPA-induced dyskinesia and rotational behaviors in the hemi-parkinsonian rat. Psychopharmacology. 2008b; 199:99–108. [PubMed: 18545986]

Dupre KB, Ostock CY, Eskow Jaunarajas KL, Button T, Savage LM, Wolf W, Bishop C. Local modulation of striatal glutamate efflux by serotonin 1A receptor stimulation in dyskinetic, hemiparkinsonian rats. Exp Neurol. 2011 in press.

Eskow KL, Gupta V, Alam S, Park JY, Bishop C. The partial 5-HT1A agonist buspirone reduces the expression and development of l-DOPA-induced dyskinesia in rats and improves l-DOPA efficacy. Pharmacol Biochem Behav. 2007; 87:306–314. [PubMed: 17553556]

Eskow KL, Dupre KB, Barnum CJ, Dickinson SO, Park JY, Bishop C. The Role of the dorsal raphe nucleus in the development, expression, and treatment of L-dopa-induced dyskinesia in hemiparkinsonian rats. Synapse. 2009; 63:610–620. [PubMed: 19309758]

Glynn G, Ahmad SO. Three-dimensional electrophysiological topography of the rat corticostriatal system. J Comp Physiol A Neuroethol Sens Neural Behav Physiol. 2002; 188:1432–1451.

Goetz CG, Damier P, Hicking C, Laska E, Muller T, Olanow CW, et al. Sarizotan as a treatment for dyskinesias in Parkinson's disease: A double-blind placebo-controlled trial. Mov Disord. 2007; 22:179–186. [PubMed: 17094088]

Hajos M, Hajos-Korscok E, Sharp T. Role of the medial prefrontal cortex in 5-HT1A receptor-induced inhibition of 5-HT neuronal activity in the rat. Br J Pharmacol. 1999; 126:1741–1750. [PubMed: 10372816]

Herrera DG, Robertson HA. Activation of c-fos in the brain. Prog Neurobiol. 1996; 50:83–107. [PubMed: 8971979]

Huot P, Johnston TH, Koprich JB, Winkelmolen L, Fox SH, Brotchie JM. Regulation of cortical and striatal 5-HT(1A) receptors in the MPTP-lesioned macaque. Neurobiol Aging. 2010 in press.

Iravani MM, Tayarani-Binazir K, Chu WB, Jackson MJ, Jenner P. In 1-methyl-4-phenyl-1,2,3,6-tetrahydropyridine-treated primates, the selective 5-hydroxytryptamine 1a agonist (R)-(+)-8-OH-DPAT inhibits levodpoa-induced dyskinesia but only with increased motor disability. J Pharmacol Exp Ther. 2006; 319:1225–1234. [PubMed: 16959959]

Jankovic J. Motor fluctuations and dyskinesias in Parkinson's disease: Clinical manifestations. Mov Disord. 2005; 20:S11–16. [PubMed: 15822109]

Jonkers N, Sarre S, Ebinger G, Michotte Y. MK801 suppresses the L-DOPA-induced increase of glutamate in striatum of hemi-Parkinsonian rats. Brain Res. 2002; 926:149–155. [PubMed: 11814417]

Lindgren HS, Andersson DR, Lagerkvist S, Nissbrandt H, Cenci MA. L-DOPA-induced dopamine efflux in the striatum and the substantia nigra in a rat model of Parkinson's disease: Temporal and quantitative relationship to the expression of dyskinesia. J Neurochem. 2010; 112(6):1465–76. [PubMed: 20050978]

Lopez A, Munoz A, Guerra MJ, Labanderia-Garcia JL. Mechanisms of the effects of exogenous levodopa on the dopamine-denervated striatum. Neuroscience. 2001; 103:639–651. [PubMed: 11274784]

Lundblad M, Anderson M, Winkler C, Kirik D, Wierup N, Cenci MA. Pharmacological validation of behavioral measures of akinesia and dyskinesia in a rat model of Parkinson's disease. Eur J Neurosci. 2002; 15:120–132. [PubMed: 11860512]

Marin C, Aguilar E, Rodriguez-Oroz MC, Bartoszyk GD, Obeso JA. Local administration of sarizotan into the subthalamic nucleus attenuates levodopa-induced dyskinesias in 6-OHDA-lesioned rats. Psychopharmacology. 2009; 204:241–250. [PubMed: 19159919]

McGeorge AJ, Faull RL. The organization of the projection from the cerebral cortex to the striatum in the rat. Neuroscience. 1989; 29(3):503–537. [PubMed: 2472578]

Mignon L, Wolf WA. Postsynaptic 5-HT1A receptors mediate an increase in locomotor activity in the monoamine-depleted rat. Psychopharmacology. 2002; 163:85–94. [PubMed: 12185404]

Mignon L, Wolf WA. 8-hydroxy-2-(di-n-propylamino)tetralin reduces striatal glutamate in an animal model of Parkinson's disease. Neuroreport. 2005; 16:699–703. [PubMed: 15858409]

Morgante F, Espay AJ, Gunraj C, Lang AE, Chen R. Motor cortex plasticity in Parkinson's disease and levodopa-induced dyskinesias. Brain. 2006; 129:1059–1069. [PubMed: 16476674]

Mura A, Mintz M, Feldon J. Behavioral and anatomical effects of long-term l-Dihydroxyphenylalanine (L-DOPA) administration in rats with unilateral lesions of the nigrostiatal system. Exp Neurol. 2002; 177:252–264. [PubMed: 12429227]

Navailles S, Benazzouz A, Bioulac B, Gross C, De Deurwaerdère P. Serotonergic neurons mediate ectopic release of dopamine induced by L-DOPA in a rat model of Parkinson's disease. Neurobiol Dis. 2010; 38:136–143. [PubMed: 20096781]

Pangalos MN, Francis PT, Foster AC, Pearson RCA, Middlemiss DN, Bowen DM. NMDA receptors assessed by autoradiography with [3H]L-689,560 are present but not enriched on corticofugal-projecting pyramidal neurons. Brain Res. 1992; 596:223–230. [PubMed: 1361417]

Paxinos, G.; Watson, W. The rat brain in stereotaxic coordinates. 4. Academic Press; San Diego: 1998.

Pompeiano M, Palacios JM, Mengod G. Distribution and cellular localization of mRNA coding for 5-HT1A receptor in the rat brain: correlation with receptor binding. J Neurosci. 1992; 12(2):440–453. [PubMed: 1531498]

Rascol O, Sabatini U, Brefel C, Fabre N, Rai S, Senard JM, et al. Cortical motor overactivation in parkinsonian patients with L-dopa-induced peak-dose dyskinesia. Brain. 1998; 121:527–533. [PubMed: 9549528]

Rektorova I, Sedlackova S, Telecka S, Hlubocky A, Rektor I. Dorsolateral prefrontal cortex: A possible target for modulating dyskinesias in Parkinson's disease by repetitive transcranial magnetic stimulation. Int J Biomed Imaging. 2008:1–6.

Robelet S, Melon C, Guillet B, Salin P, Kerkerian-Le Goff L. Chronic L-DOPA treatment increases extracellular glutamate levels and GLT1 expression in the basal ganglia in a rat model of Parkinson's disease. Eur J Neurosci. 2004; 20(5):1255–66. [PubMed: 15341597]

Sheng M, Greenberg ME. The regulation and function of c-fos and other immediate early genes in the nervous system. Neuron. 1990; 4:477–485. [PubMed: 1969743]

Soghomonian JJ. L-DOPA-induced dyskinesia in adult rats with a unilateral 6-OHDA lesion of dopamine neurons is paralleled by increased c-fos gene expression in the subthalamic nucleus. Eur J Neurosci. 2006; 23:2395–2403. [PubMed: 16706847]

Westin JE, Andersson M, Lundblad M, Cenci MA. Persistent changes in striatal gene expression induced by long-term L-DOPA treatment in a rat model of Parkinson's disease. Eur J Neurosci. 2001; 14:1171–1176. [PubMed: 11683909]

Yu H, Lewander T. Pharmacokinetic and pharmacodynamic studies of (R)¬8-hydroxy-2-(di-n-propylamino)tetralin in the rat. Eur Neuropsychopharmacol. 1997; 7:165–172. [PubMed: 9213074]

Research Highlights

- 5-HT1AR agonism with ±8-OH-DPAT reduced L-DOPA-induced AIMs and c-fos in M1.

- Site-specific microinjection of ±8-OH-DPAT into M1 reduced the onset of dyskinesia.

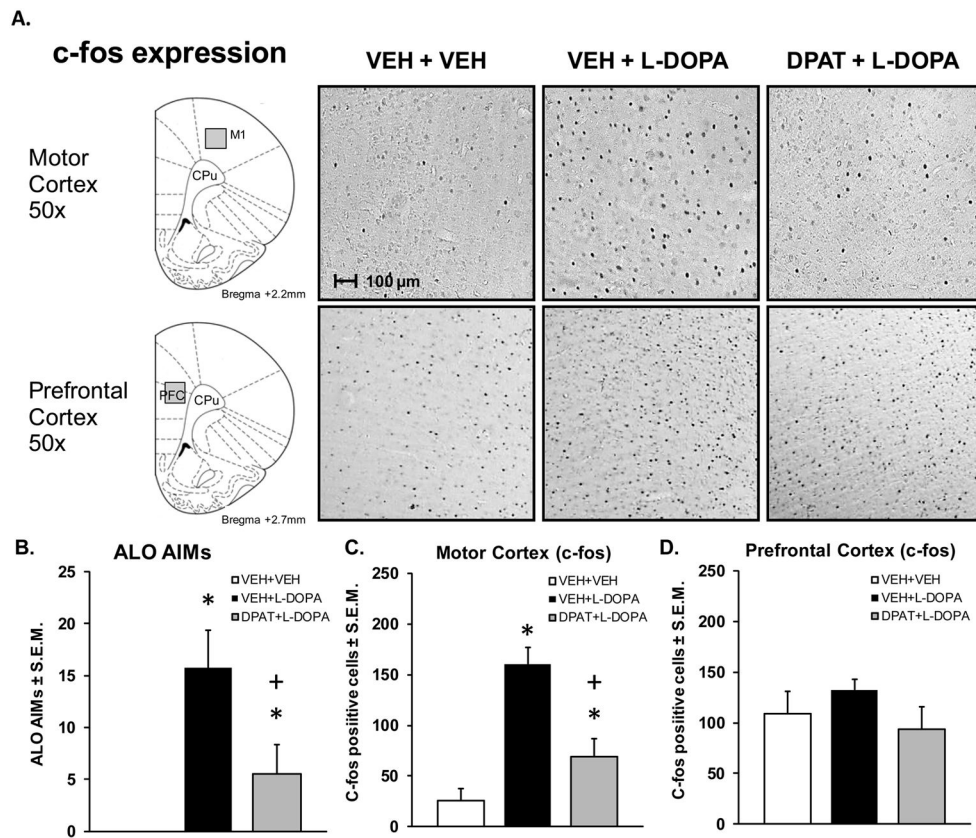- Continuous infusion of ±8-OH-DPAT into M1 reduced established dyskinesia.

Figure 1. L-DOPA-induced ALO AIMS and M1 c-fos expression are reduced by ±8-OH-DPAT
Groups of L-DOPA primed, DA depleted rats (n = 3 or 4/group) received either Vehicle
followed 5 min later by Vehicle (VEH + VEH) or L-DOPA + Benserazide (12 + 15 mg/kg,
ip; VEH + L-DOPA) or ±8-OH-DPAT (1.0 mg/kg, ip) followed by L-DOPA + Benserazide
(DPAT + L-DOPA). Rats were rated for abnormal involuntary movements (AIMs) hr after
L-DOPA treatment and then immediately perfused, after which 50 μm sections were
processed for c-fos immunohistochemistry. **(A)** Schematic depiction of motor cortex (M1)
and prefrontal cortex (PFC) analyzed for c-fos expression and photorepresentations of VEH
+ VEH, VEH + L-DOPA, DPAT + L-DOPA treatments on M1/PFC c-fos induction in DA-
depleted rats. **(B)** Bars depict mean ALO AIMs ± S.E.M. after treatment with VEH + VEH
(white), VEH + L-DOPA (black), and DPAT + L-DOPA (gray). Effects of treatments on
(C) M1 and **(D)** PFC c-fos induction, expressed as mean number of c-fos positive cells/mm^2
± S.E.M.. Treatment effects were determined by one-way ANOVA. Significant differences
for each treatment were established by post hoc planned comparisons (∗p< 0.05 vs. VEH +
VEH; +p < 0.05 vs. VEH + L-DOPA. Relevant anatomical structures: M1, primary motor
cortex; PFC, prefrontal cortex; CPu, caudate putamen).
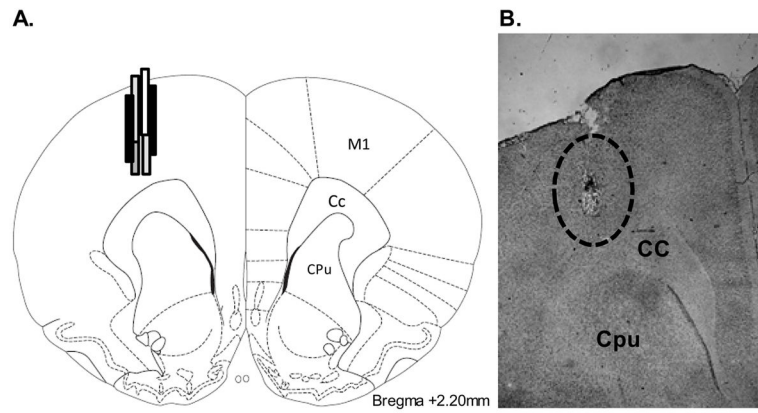
M1 Cannulation Placements

Figure 2. Cortical cannulation placements
Schematic representation **(A)** and representative cresyl violet-stained section **(B)** of M1 sections portraying typical injector placement. Schematic representation of coronal rat brain section taken from Paxinos and Watson (1998). The dashed circle depict the distribution of M1 microinfusion sites in rats used in Experiments 2 and 3. (Relevant anatomical structures: Cc, corpus callosum; Cpu, caudate putamen; M1, primary motor cortex).
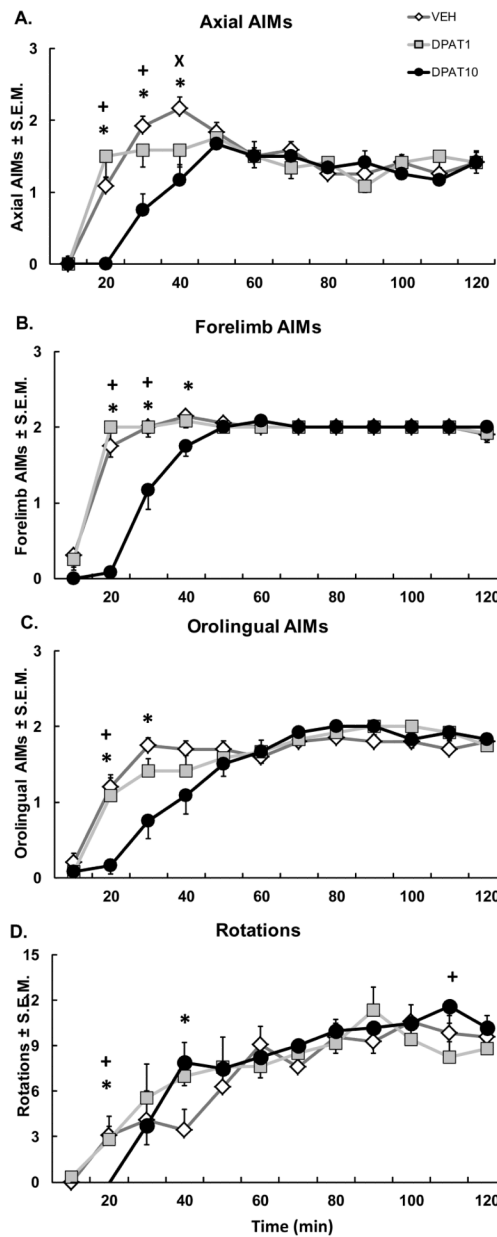
Figure 3. Intracortical ±8-OH-DPAT attenuates onset of ALO AIMs subtypes
Five min after intracortical microinfusions of Vehicle (VEH) or the 5-HT1AR agonist ±8-OH-DPAT (DPAT; 1 or 10 μg), DA depleted rats received systemic injections of L-DOPA + Benserazide (12 + 15 mg/kg, sc). Graphs depict the treatment means for **(A) A**xial, **(B)** Forelimb, and **(C)** Orolingual AIMs ± S.E.M., as well as **(D)** Rotations ± S.E.M. for 6-OHDA-lesioned rats over 2 hr of observation. Treatment effects were analyzed with Friedman ANOVAs for Axial, Forelimb, and Orolingual AIMs and two-way repeated-measures ANOVAs for Rotations. Post hoc comparisons denote significant differences between treatments at the time points indicated (*$p < 0.05$ for DPAT10 vs. VEH; ×$p < 0.05$ for DPAT1 vs. VEH; +$p < 0.05$ for DPAT10 vs. DPAT1).
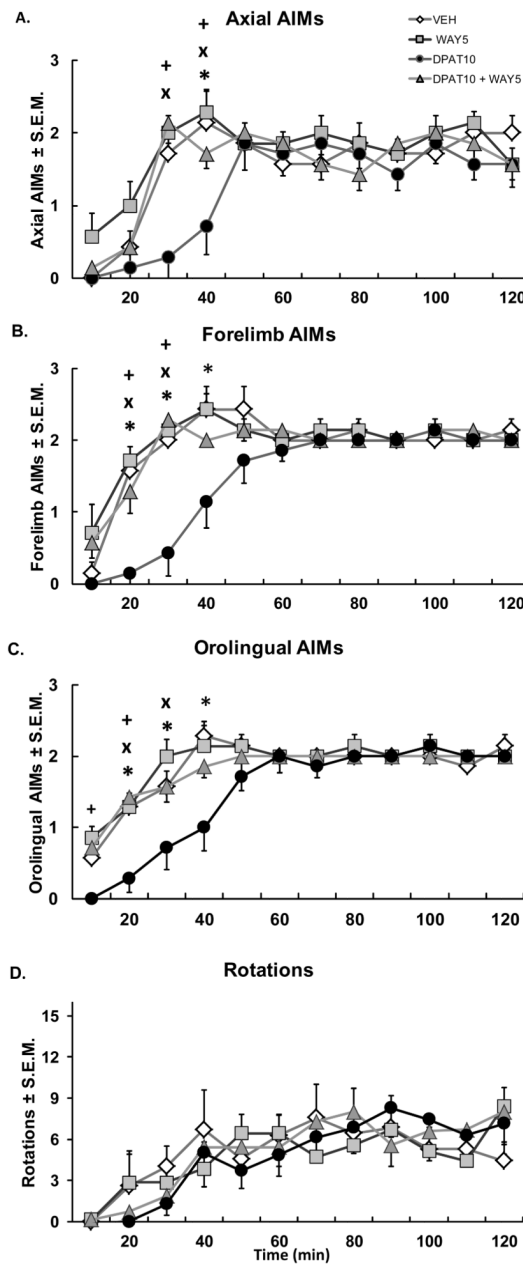
Figure 4. Co-administration of the 5-HT$_{1A}$R antagonist WAY100635 reverses ±8-OH-DPAT's anti-dyskinetic effects

Rats received intracortical microinfusions of Vehicle (VEH), the 5-HT1AR antagonist WAY100635 (5 μg; WAY5), the 5-HT$_{1A}$R agonist ±8-OH-DPAT (10 μg; DPAT10), or ±8-OH-DPAT (10 μg) + WAY100635 (5 μg; DPAT10 + WAY5), followed 5 min later by treatment with the L-DOPA + Benserazide (12 + 15 mg/kg, sc). Graphs depict treatment means for **(A)** Axial, **(B)** Forelimb, **(C)** Orolingual AIMs ± S.E.M., as well as **(D)** Rotations ± S.E.M. for 6-OHDA-lesioned rats every 10 min for 2 h. Treatment effects were determined by Friedman ANOVAs and two-way repeated-measures ANOVAs for Axial, Forelimb, and Orolingual AIMs and rotations, respectively. Post hoc comparisons indicate significant differences between treatments at the time points indicated (*p < 0.05 for

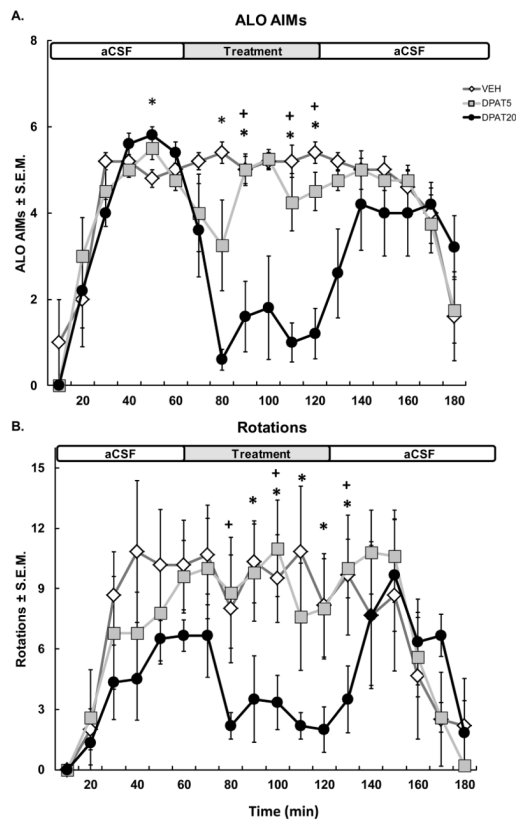DPAT10 vs VEH; ×p <0.05 for DPAT10 vs. WAY5; +p < 0.05 for DPAT10 vs. DPAT10 + WAY5).

Figure 5. Intracortical ±8-OH-DPAT reduces established ALO AIMs
Sixty min after systemic injections of L-DOPA + Benserazide (12 + 15 mg/kg, sc), VEH or ±8-OH-DPAT (DPAT; 5 & 20mM) were infused continuously into M1 for 60 min using microdialysis. Graphs depict the treatment means for **(A)** ALO AIMs ± S.E.M., as well as **(B)** Rotations ± S.E.M. for 6-OHDA-lesioned rats over 3 h of observation. Horizontal white (aCSF) and gray (treatment) bar across graph represents the timecourse of intra-M1 infusion. Treatment effects were analyzed with Kruskal-Wallis ANOVAs and two-way ANOVAs for Rotations. Post hoc comparisons denote significant differences between treatments at the time points indicated ($*p < 0.05$ for DPAT20 vs. VEH; $+p < 0.05$ for DPAT20 vs. DPAT5).